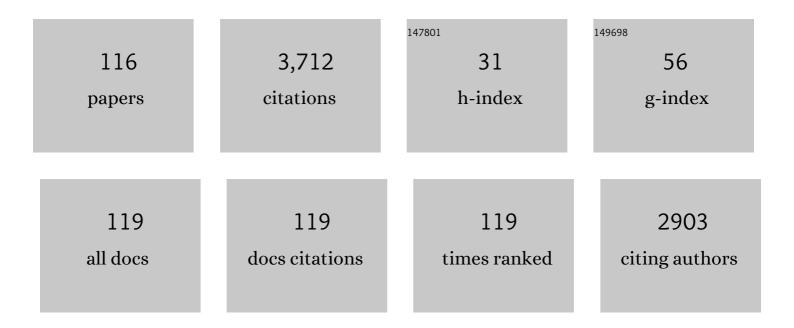
Mark A Anastasio

List of Publications by Year in descending order

Source: https://exaly.com/author-pdf/3924211/publications.pdf Version: 2024-02-01



#	Article	IF	CITATIONS
1	Imaging challenges in biomaterials and tissue engineering. Biomaterials, 2013, 34, 6615-6630.	11.4	236
2	Multiple-image radiography. Physics in Medicine and Biology, 2003, 48, 3875-3895.	3.0	219
3	Full-Wave Iterative Image Reconstruction in Photoacoustic Tomography With Acoustically Inhomogeneous Media. IEEE Transactions on Medical Imaging, 2013, 32, 1097-1110.	8.9	201
4	Investigation of iterative image reconstruction in three-dimensional optoacoustic tomography. Physics in Medicine and Biology, 2012, 57, 5399-5423.	3.0	163
5	Whole-body ring-shaped confocal photoacoustic computed tomography of small animals in vivo. Journal of Biomedical Optics, 2012, 17, 1.	2.6	143
6	An Imaging Model Incorporating Ultrasonic Transducer Properties for Three-Dimensional Optoacoustic Tomography. IEEE Transactions on Medical Imaging, 2011, 30, 203-214.	8.9	136
7	Half-time image reconstruction in thermoacoustic tomography. IEEE Transactions on Medical Imaging, 2005, 24, 199-210.	8.9	113
8	Waveform inversion with source encoding for breast sound speed reconstruction in ultrasound computed tomography. IEEE Transactions on Ultrasonics, Ferroelectrics, and Frequency Control, 2015, 62, 475-493.	3.0	111
9	Photoacoustic tomography through a whole adult human skull with a photon recycler. Journal of Biomedical Optics, 2012, 17, 110506.	2.6	105
10	Application of inverse source concepts to photoacoustic tomography. Inverse Problems, 2007, 23, S21-S35.	2.0	101
11	Enhancement of photoacoustic tomography by ultrasonic computed tomography based on optical excitation of elements of a full-ring transducer array. Optics Letters, 2013, 38, 3140.	3.3	86
12	Image reconstruction in optoacoustic tomography for dispersive acoustic media. Optics Letters, 2006, 31, 781.	3.3	77
13	Aberration correction for transcranial photoacoustic tomography of primates employing adjunct image data. Journal of Biomedical Optics, 2012, 17, 066016.	2.6	77
14	Generation of anatomically realistic numerical phantoms for photoacoustic and ultrasonic breast imaging. Journal of Biomedical Optics, 2017, 22, 041015.	2.6	70
15	A survey of computational frameworks for solving the acoustic inverse problem in three-dimensional photoacoustic computed tomography. Physics in Medicine and Biology, 2019, 64, 14TR01.	3.0	69
16	Tumor glucose metabolism imaged <i>in vivo</i> in small animals with whole-body photoacoustic computed tomography. Journal of Biomedical Optics, 2012, 17, 0760121.	2.6	62
17	High-resolution transcriptional and morphogenetic profiling of cells from micropatterned human ESC gastruloid cultures. ELife, 2020, 9, .	6.0	62
18	An extended diffraction-enhanced imaging method for implementing multiple-image radiography. Physics in Medicine and Biology, 2007, 52, 1923-1945.	3.0	55

#	Article	IF	CITATIONS
19	Accelerating image reconstruction in three-dimensional optoacoustic tomography on graphics processing units. Medical Physics, 2013, 40, 023301.	3.0	53
20	Effects of Different Imaging Models on Least-Squares Image Reconstruction Accuracy in Photoacoustic Tomography. IEEE Transactions on Medical Imaging, 2009, 28, 1781-1790.	8.9	51
21	Investigation of the far-field approximation for modeling a transducer's spatial impulse response in photoacoustic computed tomography. Photoacoustics, 2014, 2, 21-32.	7.8	48
22	Label-free photoacoustic tomography of whole mouse brain structures ex vivo. Neurophotonics, 2016, 3, 1.	3.3	47
23	Automated contouring error detection based on supervised geometric attribute distribution models for radiation therapy: A general strategy. Medical Physics, 2015, 42, 1048-1059.	3.0	45
24	Image reconstruction in photoacoustic tomography with variable speed of sound using a higher-order geometrical acoustics approximation. Journal of Biomedical Optics, 2010, 15, 021308.	2.6	39
25	Practical considerations for noise power spectra estimation for clinical CT scanners. Journal of Applied Clinical Medical Physics, 2016, 17, 392-407.	1.9	38
26	On Hallucinations in Tomographic Image Reconstruction. IEEE Transactions on Medical Imaging, 2021, 40, 3249-3260.	8.9	38
27	Investigation of discrete imaging models and iterative image reconstruction in differential X-ray phase-contrast tomography. Optics Express, 2012, 20, 10724.	3.4	34
28	Regularized Dual Averaging Image Reconstruction for Full-Wave Ultrasound Computed Tomography. IEEE Transactions on Ultrasonics, Ferroelectrics, and Frequency Control, 2017, 64, 811-825.	3.0	34
29	Deeply-supervised density regression for automatic cell counting in microscopy images. Medical Image Analysis, 2021, 68, 101892.	11.6	34
30	Photoacoustic and Thermoacoustic Tomography: Image Formation Principles. , 2011, , 781-815.		34
31	Approximating the Ideal Observer and Hotelling Observer for Binary Signal Detection Tasks by Use of Supervised Learning Methods. IEEE Transactions on Medical Imaging, 2019, 38, 2456-2468.	8.9	33
32	Analytic image reconstruction in local phase-contrast tomography. Physics in Medicine and Biology, 2004, 49, 121-144.	3.0	32
33	Assessing the Impact of Deep Neural Network-Based Image Denoising on Binary Signal Detection Tasks. IEEE Transactions on Medical Imaging, 2021, 40, 2295-2305.	8.9	32
34	Discrete Imaging Models for Three-Dimensional Optoacoustic Tomography Using Radially Symmetric Expansion Functions. IEEE Transactions on Medical Imaging, 2014, 33, 1180-1193.	8.9	31
35	3D microscopy and deep learning reveal the heterogeneity of crown-like structure microenvironments in intact adipose tissue. Science Advances, 2021, 7, .	10.3	31
36	Sparsity-regularized image reconstruction of decomposed K-edge data in spectral CT. Physics in Medicine and Biology, 2014, 59, N65-N79.	3.0	30

#	Article	IF	CITATIONS
37	Accelerated fast iterative shrinkage thresholding algorithms for sparsityâ€regularized coneâ€beam CT image reconstruction. Medical Physics, 2016, 43, 1849-1872.	3.0	30
38	Joint Reconstruction of Absorbed Optical Energy Density and Sound Speed Distributions in Photoacoustic Computed Tomography: A Numerical Investigation. IEEE Transactions on Computational Imaging, 2016, 2, 136-149.	4.4	30
39	Joint reconstruction of the initial pressure and speed of sound distributions from combined photoacoustic and ultrasound tomography measurements. Inverse Problems, 2017, 33, 124002.	2.0	29
40	Parameterized Joint Reconstruction of the Initial Pressure and Sound Speed Distributions for Photoacoustic Computed Tomography. SIAM Journal on Imaging Sciences, 2018, 11, 1560-1588.	2.2	28
41	Photoacoustic Imaging in Tissue Engineering and Regenerative Medicine. Tissue Engineering - Part B: Reviews, 2020, 26, 79-102.	4.8	28
42	Model-based optical and acoustical compensation for photoacoustic tomography of heterogeneous mediums. Photoacoustics, 2021, 23, 100275.	7.8	28
43	A Forward-Adjoint Operator Pair Based on the Elastic Wave Equation for Use in Transcranial Photoacoustic Computed Tomography. SIAM Journal on Imaging Sciences, 2017, 10, 2022-2048.	2.2	27
44	Image reconstruction in spherical-wave intensity diffraction tomography. Journal of the Optical Society of America A: Optics and Image Science, and Vision, 2005, 22, 2651.	1.5	25
45	Compensation of shear waves in photoacoustic tomography with layered acoustic media. Journal of the Optical Society of America A: Optics and Image Science, and Vision, 2011, 28, 2091.	1.5	25
46	Fast spatiotemporal image reconstruction based on low-rank matrix estimation for dynamic photoacoustic computed tomography. Journal of Biomedical Optics, 2014, 19, 1.	2.6	25
47	Iterative image reconstruction in transcranial photoacoustic tomography based on the elastic wave equation. Physics in Medicine and Biology, 2020, 65, 055009.	3.0	25
48	Feasibility of half-data image reconstruction in 3-D reflectivity tomography with a spherical aperture. IEEE Transactions on Medical Imaging, 2005, 24, 1100-1112.	8.9	23
49	A deep Boltzmann machine-driven level set method for heart motion tracking using cine MRI images. Medical Image Analysis, 2018, 47, 68-80.	11.6	23
50	Mitigation of artifacts due to isolated acoustic heterogeneities in photoacoustic computed tomography using a variable data truncation-based reconstruction method. Journal of Biomedical Optics, 2017, 22, 041018.	2.6	21
51	Two step imaging reconstruction using truncated pseudoinverse as a preliminary estimate in ultrasound guided diffuse optical tomography. Biomedical Optics Express, 2017, 8, 5437.	2.9	21
52	Treatment Outcome Prediction for Cancer Patients Based on Radiomics and Belief Function Theory. IEEE Transactions on Radiation and Plasma Medical Sciences, 2019, 3, 216-224.	3.7	21
53	A preliminary investigation of local tomography for megavoltage CT imaging. Medical Physics, 2003, 30, 2969-2980.	3.0	20
54	Reconstruction of speed-of-sound and electromagnetic absorption distributions in photoacoustic tomography. , 2006, , .		20

#	Article	IF	CITATIONS
55	Simultaneous reconstruction of speed-of-sound and optical absorption properties in photoacoustic tomography via a time-domain iterative algorithm. Proceedings of SPIE, 2008, , .	0.8	20
56	Numerical investigation of the effects of shear waves in transcranial photoacoustic tomography with a planar geometry. Journal of Biomedical Optics, 2012, 17, 061215.	2.6	20
57	Automated sleep state classification of wide-field calcium imaging data via multiplex visibility graphs and deep learning. Journal of Neuroscience Methods, 2022, 366, 109421.	2.5	18
58	Region-of-interest imaging in differential phase-contrast tomography. Optics Letters, 2007, 32, 3167.	3.3	17
59	Local cone-beam tomography image reconstruction on chords. Journal of the Optical Society of America A: Optics and Image Science, and Vision, 2007, 24, 1569.	1.5	17
60	Winner of the student award in the undergraduate category, 10th World Biomaterials Congress, May 17–22, 2016, Montreal QC, Canada: Evaluation of the tissue response to alginate encapsulated islets in an omentum pouch model. Journal of Biomedical Materials Research - Part A, 2016, 104, 1581-1590.	4.0	17
61	Recent advances in edge illumination x-ray phase-contrast tomography. Journal of Medical Imaging, 2017, 4, 1.	1.5	17
62	Xâ€ r ay phase contrast imaging of calcified tissue and biomaterial structure in bioreactor engineered tissues. Biotechnology and Bioengineering, 2015, 112, 612-620.	3.3	16
63	3-D Stochastic Numerical Breast Phantoms for Enabling Virtual Imaging Trials of Ultrasound Computed Tomography. IEEE Transactions on Ultrasonics, Ferroelectrics, and Frequency Control, 2022, 69, 135-146.	3.0	16
64	Tripling the detection view of high-frequency linear-array-based photoacoustic computed tomography by using two planar acoustic reflectors. Quantitative Imaging in Medicine and Surgery, 2015, 5, 57-62.	2.0	16
65	Gold nanorods enable noninvasive longitudinal monitoring of hydrogels in vivo with photoacoustic tomography. Acta Biomaterialia, 2020, 117, 374-383.	8.3	15
66	Single-shot edge illumination x-ray phase-contrast tomography enabled by joint image reconstruction. Optics Letters, 2017, 42, 619.	3.3	15
67	An improved reconstruction algorithm for 3-D diffraction tomography using spherical-wave sources. IEEE Transactions on Biomedical Engineering, 2003, 50, 517-521.	4.2	14
68	Analysis of ideal observer signal detectability in phase-contrast imaging employing linear shift-invariant optical systems. Journal of the Optical Society of America A: Optics and Image Science, and Vision, 2010, 27, 2648.	1.5	14
69	An integrated model-driven method for in-treatment upper airway motion tracking using cine MRI in head and neck radiation therapy. Medical Physics, 2016, 43, 4700-4710.	3.0	14
70	Compressible Latent-Space Invertible Networks for Generative Model-Constrained Image Reconstruction. IEEE Transactions on Computational Imaging, 2021, 7, 209-223.	4.4	13
71	Optimal breast cancer diagnostic strategy using combined ultrasound and diffuse optical tomography. Biomedical Optics Express, 2020, 11, 2722.	2.9	13
72	X-ray Phase Contrast Allows Three Dimensional, Quantitative Imaging of Hydrogel Implants. Annals of Biomedical Engineering, 2016, 44, 773-781.	2.5	11

#	Article	IF	CITATIONS
73	Decoding visual information from high-density diffuse optical tomography neuroimaging data. NeuroImage, 2021, 226, 117516.	4.2	11
74	Impact of deep learning-based image super-resolution on binary signal detection. Journal of Medical Imaging, 2021, 8, 065501.	1.5	11
75	Automatic CT simulation optimization for radiation therapy: A general strategy. Medical Physics, 2014, 41, 031913.	3.0	9
76	Medical image reconstruction with image-adaptive priors learned by use of generative adversarial networks. , 2020, , .		9
77	Impact of nonstationary optical illumination on image reconstruction in optoacoustic tomography. Journal of the Optical Society of America A: Optics and Image Science, and Vision, 2016, 33, 2333.	1.5	9
78	All-reflective ring illumination system for photoacoustic tomography. Journal of Biomedical Optics, 2019, 24, 1.	2.6	9
79	Normalization of optical fluence distribution for three-dimensional functional optoacoustic tomography of the breast. Journal of Biomedical Optics, 2022, 27, .	2.6	9
80	Dynamic Heterochromatin States in Anisotropic Nuclei of Cells on Aligned Nanofibers. ACS Nano, 2022, 16, 10754-10767.	14.6	9
81	Imaging of Hydrogel Microsphere Structure and Foreign Body Response Based on Endogenous X-Ray Phase Contrast. Tissue Engineering - Part C: Methods, 2016, 22, 1038-1048.	2.1	8
82	Approximating the Ideal Observer for Joint Signal Detection and Localization Tasks by use of Supervised Learning Methods. IEEE Transactions on Medical Imaging, 2020, 39, 3992-4000.	8.9	8
83	Joint reconstruction of initial pressure distribution and spatial distribution of acoustic properties of elastic media with application to transcranial photoacoustic tomography. Inverse Problems, 2020, 36, 124007.	2.0	8
84	Markov-Chain Monte Carlo approximation of the Ideal Observer using generative adversarial networks. , 2020, , .		8
85	Multispectral intensity diffraction tomography reconstruction theory: quasi-nondispersive objects. Journal of the Optical Society of America A: Optics and Image Science, and Vision, 2006, 23, 1359.	1.5	7
86	Special Section Guest Editorial: Photoacoustic Imaging and Sensing. Journal of Biomedical Optics, 2017, 22, 041001.	2.6	7
87	3D laser optoacoustic ultrasonic imaging system for research in mice (LOUIS-3DM). Proceedings of SPIE, 2014, , .	0.8	6
88	Boundary-enhancement in propagation-based x-ray phase-contrast tomosynthesis improves depth position characterization. Physics in Medicine and Biology, 2015, 60, N151-N165.	3.0	6
89	Task-based performance evaluation of deep neural network-based image denoising. , 2021, , .		5
90	A Hybrid Approach for Approximating the Ideal Observer for Joint Signal Detection and Estimation Tasks by Use of Supervised Learning and Markov-Chain Monte Carlo Methods. IEEE Transactions on Medical Imaging, 2022, 41, 1114-1124.	8.9	5

#	Article	IF	CITATIONS
91	Learning stochastic object models from medical imaging measurements by use of advanced ambient generative adversarial networks. Journal of Medical Imaging, 2022, 9, 015503.	1.5	5
92	Learning-based stochastic object models for characterizing anatomical variations. Physics in Medicine and Biology, 2018, 63, 065004.	3.0	4
93	Analysis of the Use of Unmatched Backward Operators in Iterative Image Reconstruction With Application to Three-Dimensional Optoacoustic Tomography. IEEE Transactions on Computational Imaging, 2019, 5, 437-449.	4.4	4
94	Supervised learning-based ideal observer approximation for joint detection and estimation tasks. , 2021, , .		4
95	Multispectral intensity diffraction tomography: single material objects with variable densities. Journal of the Optical Society of America A: Optics and Image Science, and Vision, 2009, 26, 403.	1.5	3
96	Reconstruction-Aware Imaging System Ranking by Use of a Sparsity-Driven Numerical Observer Enabled by Variational Bayesian Inference. IEEE Transactions on Medical Imaging, 2019, 38, 1251-1262.	8.9	3
97	A partial-dithering strategy for edge-illumination x-ray phase-contrast tomography enabled by a joint reconstruction method. Physics in Medicine and Biology, 2020, 65, 105007.	3.0	3
98	Task-based evaluation of deep image super-resolution in medical imaging. , 2021, , .		3
99	A Multivariate Functional Connectivity Approach to Mapping Brain Networks and Imputing Neural Activity in Mice. Cerebral Cortex, 2022, 32, 1593-1607.	2.9	3
100	Realistic three-dimensional optoacoustic tomography imaging trials using the VICTRE breast phantom of FDA (Conference Presentation). , 2020, , .		3
101	Elucidation of 2D and 3D photoacoustic tomography. , 2008, , .		2
102	Iterative image reconstruction in elastic inhomogenous media with application to transcranial photoacoustic tomography. Proceedings of SPIE, 2017, , .	0.8	2
103	First point-spread function and x-ray phase-contrast imaging results with an 88-mm diameter single crystal. Review of Scientific Instruments, 2018, 89, 073704.	1.3	2
104	Quantification of image texture in Xâ€ray phaseâ€contrastâ€enhanced projection images of in vivo mouse lungs observed at varied inflation pressures. Physiological Reports, 2019, 7, e14208.	1.7	2
105	Joint reconstruction of initial pressure distribution and acoustic skull parameters in transcranial photoacoustic computed tomography (Conference Presentation). , 2018, , .		2
106	Parameterized joint reconstruction of the initial pressure and sound speed distributions in photoacoustic computed tomography (Conference Presentation). , 2018, , .		2
107	Joint-reconstruction-enabled data acquisition design for single-shot edge-illumination x-ray phase-contrast tomography. , 2018, , .		2
108	Learning stochastic object model from noisy imaging measurements using AmbientGANs. , 2019, , .		2

#	Article	IF	CITATIONS
109	Progressively-Growing AmbientGANs for learning stochastic object models from imaging measurements. , 2020, , .		2
110	Computing a projection operator onto the null space of a linear imaging operator: tutorial. Journal of the Optical Society of America A: Optics and Image Science, and Vision, 2022, 39, 470.	1.5	2
111	Investigation of an elevation-focused transducer model for three-dimensional full-waveform inversion in ultrasound computed tomography. , 2022, , .		2
112	Task-based image quality assessment in radiation therapy: initial characterization and demonstration with computer-simulation study. Physics in Medicine and Biology, 2019, 64, 145020.	3.0	1
113	A signal detection model for quantifying overregularization in nonlinear image reconstruction. Medical Physics, 2021, 48, 6312-6323.	3.0	1
114	Subspace-based resolution-enhancing image reconstruction method for few-view differential phase-contrast tomography. Journal of Medical Imaging, 2018, 5, 1.	1.5	1
115	Evaluating procedures for establishing generative adversarial network-based stochastic image models in medical imaging. , 2022, , .		1
116	A learned filtered backprojection method for use with half-time circular radon transform data. , 2022, , .		0